Collision Induced Unfolding of Protein Ions in the Gas Phase Studied by Ion Mobility-Mass Spectrometry: The Effect of Ligand Binding on Conformational Stability

Jonathan T. S. Hopper and Neil J. Oldham
School of Chemistry, University of Nottingham, Nottingham, United Kingdom

Ion mobility spectrometry, with subsequent mass spectrometric detection, has been employed to study the stability of compact protein conformations of FK-binding protein, hen egg-white lysozyme, and horse heart myoglobin in the presence and absence of bound ligands. Protein ions, generated by electrospray ionization from ammonium acetate buffer, were activated by collision with argon gas to induce unfolding of their compact structures. The collisional cross sections (Ω) of folded and unfolded conformations were measured in the T-Wave mobility cell of a Waters Synapt HDMS (Waters, Altrincham, UK) employing a calibration against literature values for a range of protein standards. In the absence of activation, collisional cross section measurements were found to be consistent with those predicted for folded protein structures. Under conditions of defined collisional activation energies partially unfolded conformations were produced. The degree of unfolding and dissociation induced by these defined collision energies are related to the stability of noncovalent intra- and intermolecular interactions within protein complexes. These findings highlight the additional conformational stability of protein ions in the gas phase resulting from ligand binding. (J Am Soc Mass Spectrom 2009, 20, 1851–1858) © 2009 American Society for Mass Spectrometry

Electrospray ionization-mass spectrometry (ESI-MS) is a technique able to preserve the non-covalent interactions of protein–ligand complexes in the gas phase [1–3]. Since its original discovery, the application of ESI-MS in this area has accelerated rapidly [4, 5]. The ESI-MS approach can provide a sensitive and efficient means of obtaining valuable information relevant to binding events allowing, for example, the stoichiometries of noncovalent complexes to be easily obtained [6, 7]. The practical information available from ESI-MS measurement is already well documented [8]. In addition to stoichiometry, the affinities of protein–ligand interactions can be quantified using MS [9–12]. In many cases, binding affinities determined using ESI-MS show good agreement with values obtained using other means, potentially validating MS methods for use in early-stage screening in the drug discovery process [13, 14]. ESI-MS is not only suitable for the analysis of protein–ligand interactions, but has widespread utility in studying large protein–protein complexes [15, 16], and has been applied to the preservation and detection of very large biomolecular assemblies, including the ribosome [17, 18] and the tobacco mosaic virus (>40 MDa) [19].

A key underlying issue in ESI-MS studies of ligand binding is to what extent these findings can be related to solution behavior. Given the great importance of water to the protein fold [20], it seems clear that desolvation should result in catastrophic loss of native structure, with accompanying consequences for ligand binding. Not withstanding the role of solvation spheres around the protein, a recent study has provided evidence that an interior water molecule in FK-binding protein makes significant contribution to the structural integrity of the fold [21]. In this study, the interaction between a water molecule and the side-chain of residue E60 was investigated by obtaining high-resolution crystal structures of the wild type and two mutants (E60A and E60Q) designed to alter the interaction between water and this residue. Conclusions drawn from this study highlight that the buried water molecule is involved in a network of interactions important for the correct construction of the binding pocket. Upon desolvation, the relative strengths and importance of the noncovalent intra- and intermolecular interactions within a protein–ligand complex are altered. A recent example from the Loo group has demonstrated a clear increase in electrostatic interaction strength in the absence of water [22]. In this work, collision induced dissociation

Address reprint requests to Dr. N. J. Oldham, School of Chemistry, University of Nottingham, University Park, Nottingham, NG7 2RD, UK. E-mail: neil.oldham@nottingham.ac.uk

1044-0305/09/$32.00
doi:10.1016/j.jasms.2009.06.010

Published online July 1, 2009
Received April 14, 2009
Revised June 11, 2009
Accepted June 13, 2009

(CID) of RNase A and RNase S bound to cytidine nucleotides shows a preference for fragmentation of the covalent phosphate bond within CDP and CTP over the (noncovalent) electrostatic interaction between the phosphate residues and the RNase proteins. Earlier studies on acyl-CoA binding proteins provided evidence that, in the gas-phase, this protein-ligand interaction is driven by electrostatic forces between the CoA residue and its binding pocket, with little or no contribution from the hydrophobic acyl chain [23].

Despite these concerns, there is evidence for the (temporary) maintenance of native-like protein conformations in the mass spectrometer. In a particularly insightful experiment, the Cooks group employed the method, previously used for the analysis of viruses using mass spectrometry [24], of 'soft-landing' 8+ lysozyme ions into liquid surfaces after mass spectrometric separation [25]. The collected enzyme was shown to exhibit normal activity against hexa-N-acetylchitohexaose substrate, suggesting that the structure of lysozyme was either preserved in the gas phase, or perturbed in such a way as to allow the native fold of the enzyme to resume upon solvation. Breuker and McLafferty have recently constructed a stability timeline for desolvated protein structure from 10^{-12} to 10^{+2} s [26]. It is argued that, on the sub-50 ms timescale, the core fold is still largely intact, with the key evidence originating from the time-dependent ion mobility spectrometry work of Clemmer's group (vide infra).

The combination of ion mobility spectrometry (IMS) with mass spectrometry has emerged only relatively recently through the pioneering work of Bowers, Clemmer, Hill, Jarrold, and others, see [27] for a review, although the technique of IMS itself dates back several decades. IMS separates ions according to their charge z and collisional cross section Ω [28–30], with the latter able to provide information about biomolecular conformation in the gas-phase [31]. Thus, the combination of ESI-IMS-MS shows great promise in providing low-resolution protein structural data. The collisionally activated unfolding of cytochrome *c* in the gas phase has been studied using ESI-IMS-MS and results indicate the presence of well-defined conformations that relate to varying degrees of unfolding [31]. Similar experiments, conducted by the same group, on disulfide-intact and disulfide-reduced lysozyme have shown that the disulfide-intact protein adopts cross-sections that are in good agreement with the crystal structure. Disulfide-reduced lysozyme, in contrast, exhibits much larger conformations in the gas phase. It was also shown in this study that by introducing gas-phase proton-transfer reactions to lower the charge states observed, disulfide-reduced lysozyme shows cross sections that are indistinguishable from disulfide-intact ions [32].

To study time-dependent protein unfolding in the gas-phase, Clemmer's group have combined IMS with a Paul trap capable of trapping ions for extended time periods [33]. This study examined the 9+ charge state of cytochrome *c* over a period of 10 ms to 10 s. Results show that after 30–60 ms, the compact protein ions rapidly unfold, resulting in several highly unfolded conformation sets. On timescales between 250 ms and 10 s, these unfolded conformations proceed to refold to new, stable gas-phase conformations. The group has also used two-dimensional ion mobility (IMS/IMS) in so-called combing experiments, where narrow regions of a broader mobility distribution can be activated then passed into a second drift tube [34, 35]. These experiments have provided insights into the conformational dynamics of protein ions in the gas phase. Although broad peaks contain many unresolved smaller conformation sets, it is shown that these peaks are not due to the interconversion of smaller conformation sets, but that these structures are stable on the ~10 ms timescale of ion mobility [35].

Recent developments in IMS-MS instrumentation have seen the introduction of traveling wave mobility separators, where DC voltages are applied as a series of high-speed traveling waves in combination with rf radial confinement, allowing mobility separation without compromising MS sensitivity [36]. Ion mobility studies using such a device have demonstrated that conformations of large multiprotein complexes can be maintained upon transition to the gas phase. In one example of this, the application of IMS to the 11-membered TRAP complex, which was shown to retain its ring topology after the electrospray process, and that the binding of tryptophan aided in the preservation of this complex [37]. A more recent application of a traveling wave IMS instrument was to the analysis of active and inactive forms of the (cGMP)-dependant protein kinase by the Heck group [38]. Results obtained from this experiment suggest that the active cGMP bound protein adopts larger cross-sections than the inactive apo-protein, consistent with the expected opening of the structure implied by the HDX experiments conducted in the same study.

The present investigation was undertaken to evaluate the application of ESI-IMS-MS in studying the structural stability of compact protein ions as a function of ligand binding.

Materials and Methods

Mass Spectrometry/Ion Mobility

Electrospray ionization-ion mobility-mass spectrometry was performed on a Waters (Altrincham, UK) Synapt High Definition Mass Spectrometer (HDMS)—a hybrid quadrupole/ion mobility/orthogonal acceleration time of flight (oa-TOF) instrument. Samples were infused to the standard electrospray (z-spray) source using a Harvard (Holliston, MA, USA) apparatus 22 dual syringe pump, model 55-2222 and 100 μL Hamilton syringes (Bonaduz, Switzerland), at infusion rates between 3 and 5 μL/min. The capillary of the ESI source was typically held at voltages between 2.5 and 3 kV, with the source

operating in positive ion mode. The sample cone was operated at 10–20 V, required to avoid gas-phase unfolding and preserve non-covalent interactions. The trap T-wave collisional cell, located just before the drift tube, contained argon gas held at a pressure of 2.5×10^{-2} mbar. The ion mobility separator, containing nitrogen gas at 0.45 mbar and ambient temperature, employed a series of DC voltage waves (7 V wave height traveling at 280 m/s) to achieve conformational separation. The oa-TOF-MS was operated over the scanning range of *m/z* 500–3500 at a pressure of 1.8×10^{-6} mbar.

Sample Preparation

Lyophilized hen egg white lysozyme was obtained from Fluka (Gillingham, UK) and prepared as a 7 μM sample in 25 mM ammonium acetate solution containing 10% methanol (the presence of 10% methanol was found to improve the ESI-MS signal without significantly changing charge state distribution or ion mobility properties; see Supplementary Information Fig S1–S3, which can be found in the electronic version of this article).

The substrate of this protein, Penta-N-acetylchitopentaose (≥95%), was obtained from Sigma (Poole, UK) and prepared at 20 μM in the same buffer. To minimize the turnover of this substrate ligand, a double syringe injection system was used by infusing the protein and the ligand through separate injection lines and allowing mixing via a PEEK 'T-piece' just before the electrospray source.

Apo-myoglobin (equine heart), available as MALDI-MS standard from Sigma (Poole, UK), was acquired in 10 nmol vials. Samples of this protein (5 μM) were dissolved in 25 mM ammonium acetate solution containing 10% methanol. Holomyoglobin (equine heart) was purchased from Sigma, as a lyophilized powder ≥90% and infused in to the ESI source at a 5 μM from the same solvent.

Recombinant human FK-binding protein was acquired from Sigma as 100 μL of a 1.2 mg/mL solution. The samples were desalted using Vivaspin (Epsom, UK) columns (MWCO 3000) and diluted to 5 μM in ammonium acetate (25 mM) with 10% methanol. FK-506 monohydrate was obtained from Sigma and was added to the FKBP sample at a 6 μM final concentration.

Collisional Activation

Collisional activation was used to investigate the gas-phase stability of compact protein ion structure in the presence and absence of ligands. Activation of quadrupole isolated ions was carried out in the 'trap' region (a T-Wave cell located immediately before the ion mobility cell) of the Synapt, by collision with argon gas at 2.5×10^{-2} mbar. The resulting ion conformations were separated by the mobility cell and analyzed by TOF-MS. By adjusting the 'trap' collision energy voltage, controlling the potential offset between the source ion guide and the 'trap' region, the kinetic energies of ions entering the 'trap' could be controlled. Activation profiles were constructed from step-wise increments in collision energy applied to the 'trap' and the resulting drift traces. For all protein–ligand systems investigated here, data were acquired initially at 5 V increments, starting at 3 V. Additional, intermediate, voltages were employed between 5 V steps where major conformational change was observed. Upper voltage limits were considered to be where no further unfolding was observed. At these values, protein–ligand complexes were not fully dissociated, although partial dissociation was observed.

Kinetic Energy Considerations of CID

When investigating effects of collisionally induced activation in the gas phase, it should be appreciated that the kinetic energy (KE) of ions entering the collision cell is dependent upon their collisional cross section, with smaller ions potentially traveling at higher velocities and therefore experiencing increased collision energies. In the experiments described here, collisional activation of the ions is induced by acceleration through a relatively high vacuum region of the instrument, before entry into the 'trap' collision cell. Thus, with relatively few ion-molecule collisions, we did not anticipate significant differences in KE resulting from the minor increases (for some proteins) in cross section associated with ligand binding. To establish this, however, we measured the apparent stopping potential at the 'trap' entrance, as a measure of ion KE [39]. No detectable differences in stopping potential of the ions entering the 'trap' as a function of these small differences in collisional cross section could be observed. Therefore, in this study, any increase in an apo proteins susceptibility to unfolding does not arise from more energetic collisions.

Collisional Cross Section Calibration and Theoretical Calculations

Measured drift times were converted to collisional cross section values by calibration using proteins with known cross sections in a method similar to that previously reported [37]. Ubiquitin, cytochrome *c*, and myoglobin ions giving only single reported cross section values were used and gave a linear relationship of $\Omega/z = 72.531.(t_D^{0.52})–21.538$. Arrival times were converted to t_D by flight time correction [40]. Unless otherwise stated, CCS values for all measured proteins are reported at drift trace peak maxima. Errors in reported cross sections were determined by multiple measurements (see Supplementary Information Fig. S5). MOBCAL [41, 42] was used to obtain theoretical cross section values (Trajectory Method, TM) for native protein structures from NMR and X-ray crystal coordinates (for FKBP 1FKK, and 1FKJ, for lysozyme 1JA6 and 1SFB and for myoglobin

1MYF). For X-ray data, hydrogens were added using MolProbity [43]. The TM approach models an effective potential for the ion, based on the 12-6-4 potential of each atom, and determines the buffer gas scattering angle for orientationally-averaged collision geometries, and is taken to be a more reliable estimate of CCS for large ions.

Results and Discussion

Data Obtained from ESI-IMS-MS

Using electrospray ionization from ammonium acetate solution (25 mM, pH 6.9) the ion mobility traces and mass spectra of FK506 binding protein (FKBP), myoglobin, and lysozyme were recorded in the presence and absence of ligands, and at various degrees of collisional activation. Results are reported for the most abundant charge states observed under the conditions used. Charge states ranging from +6 to +9 were detected and similar results obtained.

FK-Binding Protein + FK-506

The ESI-mass spectrum of FKBP (5 μM) in the presence of FK-506 (6 μM) is shown in Figure 1. The charge distributions observed for both the bound and unbound protein are from 6+ to 8+, with the 7+ ions most abundant in both cases. Ion mobility drift traces obtained for apo-FKBP and the FKBP–FK-506 complex ($[M + 7H]^{7+}$ charge states) using mild operating conditions (sample cone voltage 20 V, Trap collision cell off-set voltage 10 V, the maximum value before the onset of unfolding) are presented in Figure 2. Markers are included to illustrate the average trajectory model (TM) collisional cross sections (CCSs) calculated for the natively folded conformations of these two species using MOBCAL [41, 42] and X-ray-derived structural coordinates (PDB files 1FKK and 1FKJ, respectively). The experimental CCSs (1247 and 1358 ± 11 Å^2) are in very good agreement with the theoretical values calculated at 1331 and 1387Å^2 for the apo and holo protein, respectively, suggesting that the $[M + 7H]^{7+}$ charge state ion of FKBP adopts a conformation of similar size to the folded solution species. It is apparent that, unlike the protein–ligand complex, which maintains a fairly narrow Gaussian distribution of conformations, the unbound protein shows a broad signal, with a shoulder at higher drift times (lower trap voltages, to a minimum of 3 V, did not result in markedly different drift trace distributions for any of the three proteins studied, see Supplementary Information Fig. S4). Therefore, under these mild conditions, it seems that either the FKBP–FK-506 complex shows signs of greater conformational stability and structural integrity in the gas phase, or the ligand is selecting a particular set of diverse solution conformations for binding.

Raising the 'trap' collision energy (see the Materials and Methods section) to 15 V induces conformational unfolding of both the holo- and apo-proteins, as shown in Figure 2. Apo-FKBP largely adopts a more unfolded conformation around 1500 Å^2, with only a small population of compact protein ions. This is evident to a lesser extent for the FKBP–FK-506 complex, where the majority of the ions present retain compact CCSs with only a relatively small population of unfolded species at ~1560Å^2. At 20 V (Figure 2), both the holo and apo species are almost exclusively present in single partially unfolded states. The offset of the apo and holo peaks is ~67 Å^2, which is of similar magnitude to the theoretical cross section added due to the presence of the ligand (~56 Å^2) calculated from the difference between the calculated holo and apo native CSSs. Further increase in trap collision energy to 25 V induces further conformational unfolding (Figure 2). Here, there is a clear lag in

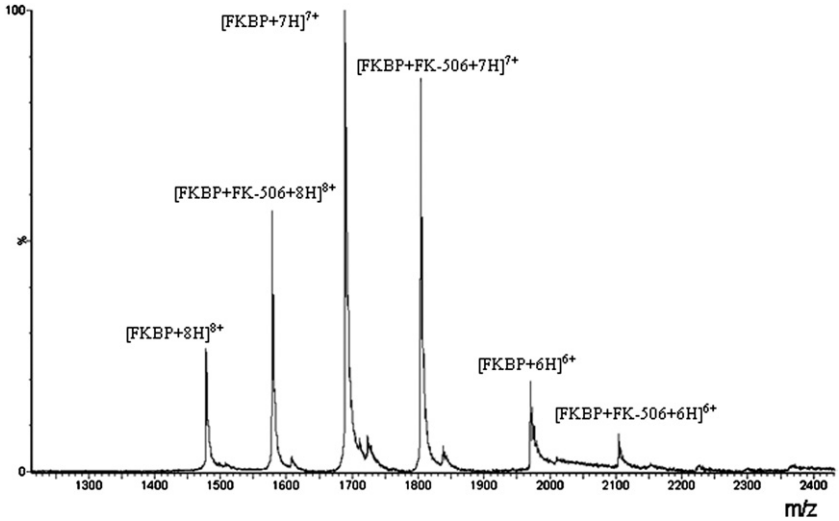

Figure 1. ESI-MS spectrum of FKBP (5 μM) in the presence of FK506 (6 μM) showing the distributions of 8+ to 6+ ions of both the FKBP and the FKBP + FK-506 complex.

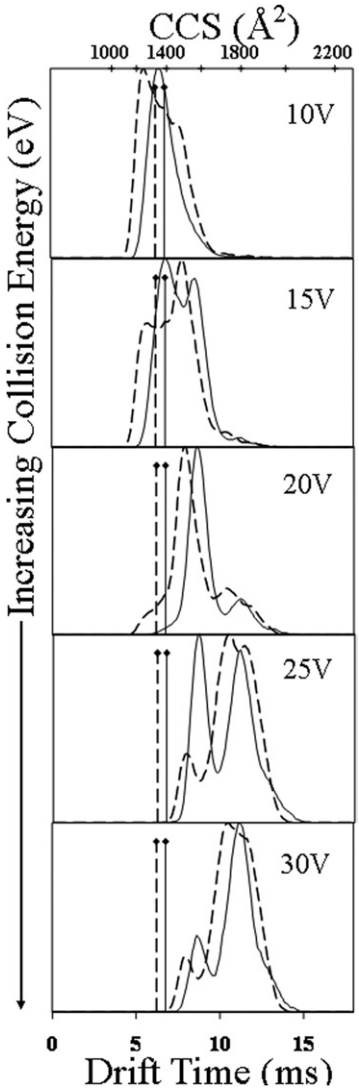

Figure 2. The unfolding profile of the $[FKBP + 7H]^{7+}$ (dashed trace) and the $[FKBP + FK\text{-}506 + 7H]^{7+}$ (solid trace). The dashed and solid markers indicate the calculated theoretical cross sections for the apo and holo ions as obtained using MOBCAL.

the degree of unfolding observed for the FKBP–FK-506 complex, relative to the unbound FKBP. Conformations observed for FKBP–FK-506 at this voltage show ion populations that are split almost equally between the 1560 Å^2 conformation, observed previously at a trap voltage of 20 V, and a new distribution of conformations at ~1790 Å^2. The apo protein however retains only a small population at smaller CCS and mainly adopts what appears to be two poorly resolved conformation sets at 1730 and 1810 Å^2. Increasing the collision energy to 30 V sees the holo $[FKBP–FK\text{-}506]^{7+}$ adopt primarily the most unfolded conformation observed for this complex at ~1790 Å^2. The drift trace of the apo-FKBP at this energy appears essentially unchanged from its conformation distribution at the previous energy of 25 V, suggesting that this too has reached a maximum CCS (with higher collision energies inducing no further unfolding).

Lysozyme + Penta-N-Acetylchitopentaose

The lysozyme–NAG_5 noncovalent complex exhibits an unfolding effect similar to that observed for FKBP. However, here the 8+ charge state shows only one major structural rearrangement which occurs over a very narrow collision energy range. This is attributed to the disulfide linkages, which stabilize the protein core also seen in previous work on unliganded lysozyme [32]. The drift trace at 10 V (Figure 3) shows that both the holo- and apo-species at low activation energies exhibit CCSs similar to calculated theoretical values (measured 1487 and 1408 ± 44 Å^2; calculated 1567 and 1644Å^2 for lysozyme and lysozyme–NAG_5 respectively). The agreement between experimental and theoretical values for apo-lysozyme (~5.1%) is significantly better than the holo-lysozyme (~14.4%). It is notable that the measured CSS of lysozyme–NAG_5 (taken at the maximum peak intensity) is smaller than that of lysozyme alone, suggesting a higher degree of structural collapse may be present here. The theoretical cross sections are still within the boundaries of these

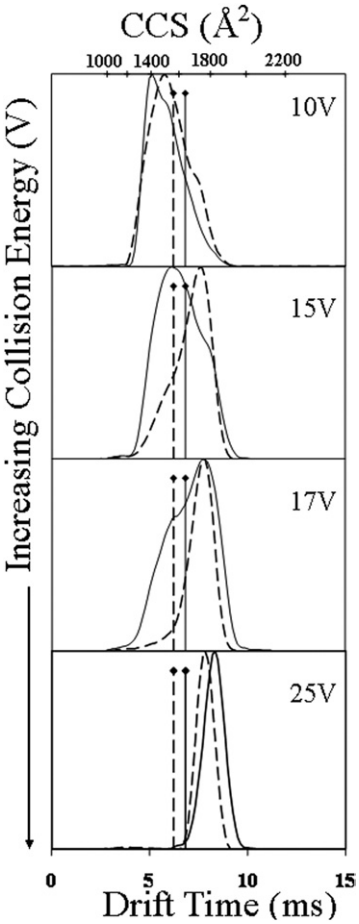

Figure 3. The unfolding profile of the $[Lysozyme + 8H]^{8+}$ (dashed trace) and the $[Lysozyme + NAG_5 + 8H]^{8+}$ (solid trace). The dashed and solid markers indicate the calculated theoretical cross sections for the apo and holo ions as obtained using MOBCAL.

broad peaks, however. The cross section of 6+ apo-lysozyme has been determined previously by traveling wave IMS by Smith et al. and is reported as 1333 Å^2 [44], demonstrating yet further collapse in this lower charge state.

When the collision energy is raised to 15 V, a major conformational shift of the unbound protein can be observed, gaining ~240 Å^2 in CCS. The bound protein–substrate system also undergoes a small increase in collisional cross section (~150 Å^2), however, the degree of unfolding induced is clearly not as extensive. Raising the energy by just 2 V (to 17 V in Figure 3) induces sufficient unfolding of the lysozyme–NAG_5 complex to produce a comparable cross section to the apo-protein. The shoulder at lower drift times on the holo-trace shows that populations of more compact conformations are still present. This 'lag' in unfolding demonstrates that, as with the FKBP–FK-506 protein system, the additional intermolecular interactions from the ligand appear to provide a stabilizing effect on the compact protein structure. At the highest 'trap' collision energy shown, the drift traces for both lysozyme and lysozyme–NAG_5 show very narrow Gaussian peaks, with the enzyme–substrate complex exhibiting a larger (60 Å^2) CSS than lysozyme alone, perhaps resulting from externalization of the ligand. As the protein fold is disrupted, and the NAG_5 contacts with lysozyme are reduced, producing a conformationally flexible entity, which adds significantly to the cross section. This result is in distinct contrast to the data measured at low-energy.

Holo-Myoglobin + Apo-Myoglobin

To provide further evidence for this effect, measurements were also conducted on the 8+ charge state of holo- and apo-horse heart myoglobin. Smith et al. have previously reported the cross section for the 6+ charge state of horse heart myoglobin measured using a traveling wave IMS to be 1314 Å^2 [44]. Theoretical calculation of CSS using MOBCAL was only possible for the holo-form of the protein, since the high-resolution structure for apo-myoglobin has not been obtained. From Figure 4, at 10 V, the trace representing the holo-myoglobin is in excellent agreement with the calculated value (measure value 1742 ± 46 Å^2; calculated value 1781 Å^2). To induce major unfolding in this system, the collision energy was raised to 20 V where a high degree of unfolding for the apo-protein into a complex set of conformations is apparent. The effect of this degree of activation on the holomyoglobin is much less pronounced. Larger conformations are adopted, but to a much lesser extent and are only apparent as higher CCS shoulders on the existing drift trace. At 25 V, holomyoglobin unfolds extensively, although it still possesses more compact conformations than the apo-protein. At 30 V, both holo- and apo-myoglobin reach their limit of unfolding and produce narrow, near-identical conformer distributions around 2512 Å^2.

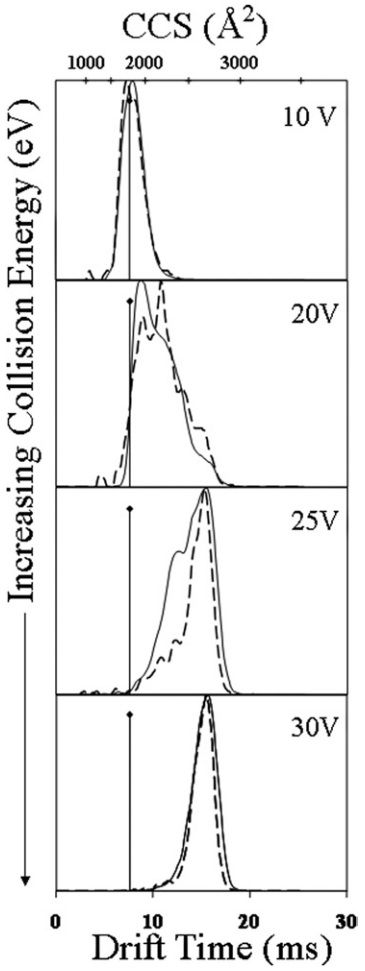

Figure 4. The unfolding profile of the [Apomyoglobin + 8H]$^{8+}$ (dashed trace) and the [Myoglobin + 8H]$^{8+}$ (solid trace). The solid marker indicates the calculated theoretical cross section for myoglobin as obtained using MOBCAL.

Quantification of Protein–Ligand Complex Unfolding and Dissociation in the Gas Phase

To derive descriptive values for the stability of protein–ligand complexes with respect to both unfolding and dissociation (loss of the ligand), we determined the E_{lab} energies required to induce 50% unfolding or 50% dissociation of the complexes. To obtain the unfolding values, $Ec_{50(unfold)}$, the energy required to induce conformations half way between the minimum and maximum cross sections observed was measured. The collision energies required to induce 50% dissociation, $Ec_{50(diss)}$, were measured by plotting disappearance of precursor as a function of E_{lab} collision energy and the 50% value read from the resulting sigmoid plots (see Supplementary Information Fig. S6 and S7 for an example). The results are provided in Table 1. Comparison of the $Ec_{50(unfold)}$ values for the three apo-proteins and their protein–ligand complexes reveals a significant increase in value upon ligand binding in each case ($\Delta Ec_{50(unfold)}$ of 9 eV, 21 eV, and 7 eV for FKBP, lysozyme, and myoglobin respectively). Thus, as indi-

Table 1. Ec_{50} values for the unfolding and dissociation of FKBP, lysozyme, and myoglobin ions. Also quoted are estimates of the internal energies, ΔE_{int}, gained by each ion at these Ec_{50} points

Protein	$Ec_{50(unfold)}$/eV	$\Delta E_{int(unfold)}$/eV	$Ec_{50(diss)}$/eV	$\Delta E_{int(diss)}$/eV
FKBP	118	49.3	—	—
FKBP.FK506	127	53.1	198	84.9
Lysozyme	114	46.3	—	—
Lysozyme.NAG_5	135	55.3	378	171
Apomyoglobin	160	66.1	—	—
Holomyoglobin	167	69.1	420	188

cated by the drift traces in Figures 2, 3, and 4, the presence of a bound ligand leads to an increased resistance to gas-phase unfolding of the protein ions. For each protein the $Ec_{50(unfold)}$ values for both apo- and holo-proteins are significantly less than the $Ec_{50(diss)}$ for dissociation of the complex (Table 1). FKBP exhibits the smallest difference between $Ec_{50(unfold)}$ and $Ec_{50(diss)}$ at 71 eV, and myoglobin the greatest at 253 eV. It would appear, therefore that unfolding precedes dissociation under conditions of low-energy multiple collision induced activation. It should be borne in mind that $Ec_{50(unfold)}$, as expressed here, represents a measure of the observed extent of unfolding for the major charge states of each protein, and not the absolute unfolded state. Refolding processes during, or immediately before, ion mobility cannot be ruled out, although see [34].

E_{lab} collision energy values, defined by acceleration voltage and resulting ion kinetic energy, provide only an indirect measure of protein–ligand complex stability. A more direct description is given by determining the internal energy gained as a result of multiple low-energy collisions. Douglas has developed a model [39, 45] to describe this phenomenon in a quadrupole collision cell. Whilst the traveling wave collision cell employed in this study is not a quadrupole environment, the approach still permits an estimation of the relative increase in ion internal energy, ΔE_{int}, upon collision with a neutral gas, especially as the T-wave parameters (wave height, velocity, entrance, and exit voltages) were kept constant throughout the experiments. Estimates of internal energies gained by the protein ions at collision energies required to give 50% unfolding of both the holo and apo species have been calculated from $Ec_{50(unfold)}$ (Table 1). Expressed as $\Delta\Delta E_{int(unfold)}$, values for FK-binding protein, lysozyme, and myoglobin are 3.84, 9.04, and 2.96 eV respectively. These values exhibit a similar trend to the $Ec_{50(unfold)}$ data, from which they are derived, but represent a more accurate measure of the relative additional stability afforded by the presence of the ligand. In the case of FKBP we also determined the increase in stability of the protein fold upon FK506 binding in solution using stability of unpurified proteins from rates of H/D exchange (SUPREX) [46]. The decrease in Gibbs free-energy for folding due to the presence of FK506 ($\Delta\Delta G_f$) was determined to be -4.62 kcal mol^{-1} (details to be reported elsewhere). Thus, as expected, the protein fold in solution is stabilized by ligand binding. Our results show that this effect is also apparent in the gas phase, for the three proteins investigated, under conditions of collisional activation.

Acknowledgments

The authors gratefully acknowledge to Dr. Kevin Giles of Waters for helpful discussions, and the University of Nottingham for financial support.

Appendix A Supplementary Material

Supplementary material associated with this article may be found in the online version at doi:10.1016/j.jasms.2009.06.010.

References

1. Ganem, B.; Li, Y. T.; Henion, J. D. Detection of Noncovalent Receptor Ligand Complexes by Mass-Spectrometry. *J. Am. Chem. Soc.* **1991,** *113*, 6294–6296.
2. Ganem, B.; Li, Y. T.; Henion, J. D. Observation of Noncovalent Enzyme Substrate and Enzyme Product Complexes by Ion-Spray Mass-Spectrometry. *J. Am. Chem. Soc.* **1991,** *113*, 7818–7819.
3. Katta, V.; Chait, B. T. Observation of the Heme Globin Complex in Native Myoglobin by Electrospray-Ionization Mass-Spectrometry. *J. Am. Chem. Soc.* **1991,** *113*, 8534–8535.
4. Loo, J. A. Studying Noncovalent Protein Complexes by Electrospray Ionization Mass Spectrometry. *Mass Spectrom. Rev.* **1997,** *16*, 1–23.
5. Sinz, A. Investigation of Protein–Ligand Interactions by Mass Spectrometry. *Chem. Med. Chem.* **2007,** *2*, 425–431.
6. Kouvatsos, N.; Thurston, V.; Ball, K.; Oldham, N. J.; Thomas, N. R.; Searle, M. S. Bile Acid Interactions with Rabbit Ileal Lipid Binding Protein and an Engineered Helixless Variant Reveal Novel Ligand Binding Properties of a Versatile β-Clam Shell Protein Scaffold. *J. Mol. Biol.* **2007,** *371*, 1365–1377.
7. Oldham, N. J.; Lissina, O.; Nunn, M. A.; Paesen, G. C. Nondenaturing Electrospray Ionization-Mass Spectrometry Reveals Ligand Selectivity in Histamine-Binding Protein RaHBP2. *Org. Biomol. Chem.* **2003,** *1*, 3645–3646.
8. Sobott, F.; Robinson, C. V. Protein Complexes Gain Momentum. *Curr. Opin. Struc. Biol.* **2002,** *12*, 729–734.
9. Veros, C. T.; Oldham, N. J. Quantitative Determination of Lysozyme–Ligand Binding in the Solution and Gas Phases by Electrospray Ionization Mass Spectrometry. *Rapid Commun. Mass Spectrom.* **2007,** *21*, 3505–3510.
10. Mathur, S.; Badertscher, M.; Scott, M.; Zenobi, R. Critical Evaluation of Mass Spectrometric Measurement of Dissociation Constants: Accuracy and Cross-validation against Surface Plasmon Resonance and Circular Dichroism for the Calmodulin-Melittin System. *Phys. Chem. Phys.* **2007,** *9*, 6187–6198.
11. Jecklin, M. C.; Touboul, D.; Bovet, C.; Wortmann, A.; Zenobi, R. Which Electrospray-Based Ionization Method Best Reflects Protein–Ligand Interactions Found In Solution? A Comparison of ESI, NanoESI, and ESSI for the Determination of Dissociation Constants with Mass Spectrometry. *J. Am. Soc. Mass Spectrom.* **2008,** *19*, 1237–1237.
12. Wortmann, A.; Jecklin, M. C.; Touboul, D.; Badertscher, M.; Zenobi, R. Binding Constant Determination of High-Affinity Protein–Ligand Complexes by Electrospray Ionization Mass Spectrometry and Ligand Competition. *J. Mass Spectrom.* **2008,** *43*, 600–608.
13. Vu, H.; Quinn, R. J. Direct Screening of Natural Product Extracts Using Mass Spectrometry. *J. Biomol. Screen.* **2008,** *13*, 265–275.

14. Poulsen, S. A. Direct Screening of a Dynamic Combinatorial Library Using Mass Spectrometry. *J. Am. Soc. Mass Spectrom.* **2006,** *17*, 1074–1080.
15. Zhou, M.; Sandercock, A. M.; Fraser, C. S.; Ridlova, G.; Stephens, E.; Schenauer, M. R.; Yokoi-Fong, T.; Barsky, D.; Leary, J. A.; Hershey, J. W.; Doudna, J. A.; Robinson, C. V. Mass Spectrometry Reveals Modularity and a Complete Subunit Interaction Map of the Eukaryotic Translation Factor eIF3. *Proc. Natl. Acad. Sci. U.S.A.* **2008,** *105*, 18139–18144.
16. Geels, R. B. J.; Calmat, S.; Heck, A. J. R.; van der Vies, S. M.; Heeren, R. M. A. Thermal Activation of the Cochaperonins GroES and gp31 Probed by Mass Spectrometry. *Rapid Commun. Mass Spectrom.* **2008,** *22*, 3633–3641.
17. Videler, H.; Ilag, L. L.; McKay, A. R. C.; Hanson, C. L.; Robinson, C. V. Mass Spectrometry of Intact Ribosomes. *Proceedings of the 130th Nobel Symposium on Molecular Mechanisms in Biological Processes*; Tallberg, Sweden, September 2004. Elsevier Science.
18. Rostom, A. A.; Fucini, P.; Benjamin, D. R.; Juenemann, R.; Nierhaus, K. H.; Hartl, F. U.; Dobson, C. M.; Robinson, C. V. Detection and Selective Dissociation of Intact Ribosomes in a Mass Spectrometer. *Proc. Natl. Acad. Sci. U.S.A.* **2000,** *97*, 5185–5190.
19. Bothner, B.; Siuzdak, G. Electrospray Ionization of a Whole Virus: Analyzing Mass, Structure, and Viability. *Chem. BioChem.* **2004,** *5*, 258–260.
20. Chaplin, M. Opinion—Do We Underestimate the Importance of Water in Cell Biology? *Nature Rev. Mol. Cell Biol.* **2006,** *7*, 861–866.
21. Szep, S.; Park, S.; Boder, E. T.; Van Duyne G. D.; Saven, J. G. Structural Coupling Between FKBP12 and Buried Water. *Prot. Struct. Funct. Bioinformat.* **2009,** *74*, 603–611.
22. Yin, S.; Xie, Y. M.; Loo, J. A. Mass Spectrometry of Protein-ligand Complexes: Enhanced Gas-Phase Stability of Ribonuclease–Nucleotide complexes. *J. Am. Soc. Mass Spectrom.* **2008,** *19*, 1199–1208.
23. Robinson, C.; Chung, E.; Kragelund, B.; Knudsen, J.; Aplin, R.; Poulsen, F.; Dobson, C. Probing the Nature of Noncovalent Interactions by Mass Spectrometry. A Study of Protein–CoA Ligand Binding and Assembly. *J. Am. Chem. Soc.* **1996,** *118*, 8646–8653.
24. Siuzdak, G.; Bothner, B.; Yeager, M.; Brugidou, C.; Fauquet, C. M.; Hoey, K.; Chang, C. M. Mass Spectrometry and Viral Analysis. *Chem. Biol.* **1996,** *3*, 45–48.
25. Gologan, B.; Takats, Z.; Alvarez, J.; Wiseman, J. M.; Talaty, N.; Ouyang, Z.; Cooks, R. G. Ion Soft-Landing into Liquids: Protein Identification, Separation, and Purification with Retention of Biological Activity. *J. Am. Soc. Mass Spectrom.* **2004,** *15*, 1874–1884.
26. Breuker, K.; McLafferty, F. Stepwise Evolution of Protein Native Structure with Electrospray into the Gas Phase, 10^{-12} to 10^{2} s. *Proc. Natl. Acad. Sci. U.S.A.* **2008,** *105*, 18145–18152.
27. Kanu, A. B.; Dwivedi, P.; Tam, M.; Matz, L.; Hill, H. H. Ion Mobility-Mass Spectrometry. *J. Mass Spectrom.* **2008,** *43*, 1–22.
28. Karasek, F. W. Plasma Chromatography. *Anal. Chem.* **1974,** *46*, A710–A720.
29. Viehland, L. A.; Mason, E. A. Transport Properties of Gaseous-Ions Over a Wide Energy-Range. *Atomic Data Nuclear Data Tables* **1995,** *60*, 37–95.
30. Creaser, C. S.; Griffiths, J. R.; Bramwell, C. J.; Noreen, S.; Hill, C. A.; Thomas, C. L. P. Ion Mobility Spectrometry: A Review. Part 1. Structural Analysis by Mobility Measurement. *Analyst* **2004,** *129*, 984–994.
31. Clemmer, D. E.; Hudgins, R. R.; Jarrold, M. F. Naked Protein Conformations—Cytochrome *c* in the Gas Phase. *J. Am. Chem. Soc.* **1995,** *117*, 10141–10142.
32. Valentine, S. J.; Anderson, J. G.; Ellington, A. D.; Clemmer, D. E. Disulfide-Intact and -Reduced Lysozyme in the Gas Phase: Conformations and Pathways of Folding and Unfolding. *J. Phys. Chem. B* **1997,** *101*, 3891–3900.
33. Badman, E. R.; Myung, S.; Clemmer, D. E. Evidence for Unfolding and Refolding of Gas-Phase Cytochrome *c* Ions in a Paul Trap. *J. Am. Soc. Mass Spectrom.* **2005,** *16*, 1493–1497.
34. Koeniger, S. L.; Merenbloom, S. I.; Clemmer, D. E. Evidence for Many Resolvable Structures within Conformation Types of Electrosprayed Ubiquitin Ions. *J. Phys. Chem. B* **2006,** *110*, 7017–7021.
35. Merenbloom, S. I.; Koeniger, S. L.; Bohrer, B. C.; Valentine, S. J.; Clemmer, D. E. Improving the Efficiency of IMS-IMS by a Combing Technique. *Anal. Chem.* **2008,** *80*, 1918–1927.
36. Pringle, S. D.; Giles, K.; Wildgoose, J. L.; Williams, J. P.; Slade, S. E.; Thalassinos, K.; Bateman, R. H.; Bowers, M. T.; Scrivens, J. H. An Investigation of the Mobility Separation of Some Peptide and Protein Ions Using a New Hybrid Quadrupole/Traveling Wave IMS/Oa-TOF Instrument. *Int. J. Mass Spectrom.* **2007,** *261*, 1–12.
37. Ruotolo, B. T.; Giles, K.; Campuzano, I.; Sandercock, A. M.; Bateman, R. H.; Robinson, C. V. Evidence for Macromolecular Protein Rings in the Absence of Bulk Water. *Science* **2005,** *310*, 1658–1661.
38. Alverdi, V.; Mazon, H.; Versluis, C.; Hemrika, W.; Esposito, G.; van den Heuvel, R.; Scholten, A.; Heck, A. J. R. cGMP-binding Prepares PKG for Substrate Binding by Disclosing the C-Terminal Domain. *J. Mol. Biol.* **2008,** *375*, 1380–1393.
39. Covey, T.; Douglas, D. J. Collision Cross-Sections for Protein Ions. *J. Am. Soc. Mass Spectrom.* **1993,** *4*, 616–623.
40. Thalassinos, K.; Slade, S. E.; Jennings, K. R.; Scrivens, J. H.; Giles, K.; Wildgoose, J.; Hoyes, J.; Bateman, R. H.; Bowers, M. T. Ion Mobility Mass Spectrometry of Proteins in a Modified Commercial Mass Spectrometer. *Int. J. Mass Spectrom.* **2004,** *236*, 55–63.
41. Shvartsburg, A. A.; Jarrold, M. F. An Exact Hard-Spheres Scattering Model for the Mobilities of Polyatomic Ions. *Chem. Phys. Lett.* **1996,** *261*, 86–91.
42. Mesleh, M. F.; Hunter, J. M.; Shvartsburg, A. A.; Schatz, G. C.; Jarrold, M. F. Structural Information from Ion Mobility Measurements: Effects of the Long-Range Potential. *J. Phys. Chem. A* **1996,** *100*, 16082–16086.
43. Davis, I. W.; Leaver-Fay, A.; Chen, V. B.; Block, J. N.; Kapral, G. J.; Wang, X.; Murray, L. W.; Arendall, W. B.; Snoeyink, J.; Richardson, J. S.; Richardson, D. C. MolProbity: All-Atom Contacts and Structure Validation for Proteins and Nucleic Acids. *Nucleic Acids Res.* **2007,** *35*, W375–W383.
44. Smith, D. P.; Knapman, T. W.; Campuzano, I.; Malham, R. W.; Berryman, J. T.; Radford, S. E.; Ashcroft, A. E. Deciphering Drift Time Measurements from Traveling Wave Ion Mobility Spectrometry-mass Spectrometry Studies. *Eur. J. Mass Spectrom.* **2009,** *15*, 113–130.
45. Mark, K. J.; Douglas, D. J. Coulomb Effects in Binding of Heme in Gas-Phase Ions of Myoglobin. *Rapid Commun. Mass Spectrom.* **2006,** *20*, 111–117.
46. Ghaemmaghami, S.; Fitzgerald, M.; Oas, T. A Quantitative, High-Throughput Screen for Protein Stability. *Proc. Natl. Acad. Sci. U.S.A.* **2000,** *97*, 8296–8301.